Journal of Materials Chemistry C

RSC Publishing

PAPER

View Article Online
View Journal | View Issue

Cite this: J. Mater. Chem. C, 2013, 1, 7709

Hybrid hierarchical patterns of gold nanoparticles and poly(ethylene glycol) microstructures†

Jingyu Chen,‡[a] Manar Arafeh,[a] Amandine Guiet,[b] Diana Felkel,[b] Axel Loebus,[a] Susan M. Kelleher,§[a] Anna Fischer[b] and Marga C. Lensen*[a]

Received 30th April 2013
Accepted 17th July 2013

DOI: 10.1039/c3tc30811a

www.rsc.org/MaterialsC

Hybrid surface micro-patterns composed of topographic structures of polyethylene glycol (PEG)-hydrogels and hierarchical lines of gold nanoparticles (Au NPs) were fabricated on silicon wafers. Micro-sized lines of Au NPs were first obtained on the surface of a silicon wafer *via* "micro-contact deprinting", a method recently developed by our group. Topographic micro-patterns of PEG, of both low and high aspect ratio (AR up to 6), were then aligned on the pre-patterned surface *via* a procedure adapted from the soft lithographic method MIMIC (Micro-Molding in Capillaries), which is denoted as "adhesive embossing". The result is a complex surface pattern consisting of alternating flat Au NP lines and thick PEG bars. Such patterns provide novel model surfaces for elucidating the interplay between (bio)chemical and physical cues on cell behavior.

Introduction

The interaction between cells and the surface of natural and artificial biomaterials has been a focus of much research in recent decades and the information gained is of great significance for the development of tissue engineering and biomedicine.[1] Cell culture substrates with micro-sized chemical and topographical patterns have also been widely investigated in this area, since cell adhesion and subsequent processes, such as spreading, migration and proliferation, have been shown to be critically dependent on chemical and physical cues at the bio-interface. Several reports on the methods used to form patterned polymer surfaces have been published, including photolithography,[2–6] plasma pattern writing,[7] and soft-lithography techniques such as micro-contact printing,[8] replica molding[9,10] and Micro-Molding in Capillaries (MIMIC).[11] However, most of the patterning methods reported so far have only provided single cues to cells, such as either two-dimensional (2D) chemical patterns on flat surfaces, or topographic patterns fabricated on uniform materials. With the research on cell behavior at the bio-interface marching ahead, it is obvious that such simple patterns are not sufficient to meet the aim of imitating the complexity of the three-dimensional (3D) *in vivo* environment, in which cells face a multitude of (bio)chemical and physical factors.

Therefore, we designed novel, hierarchically patterned surfaces, exhibiting bi-functional patterns, consisting of (1) micro-sized physical barriers of a cell anti-adhesive material teamed with (2) nano-sized chemical anchoring points for bio-functional molecules in order to produce an advanced platform with multiple (micro- and nano-sized) cues for fundamental cell studies. In such bi-functional patterns, the physical barriers are formed by micrometer-sized topographic structures consisting of polyethylene glycol (PEG) bars with variable aspect ratios while the nanoscopic (bio-)chemical pattern (*e.g.* composed of cell adhesion mediating molecules that are linked to the gold nanostructures *via* thiol-gold chemistry) can be established by means of the ordered deposition of Au NPs on the substrate.

Polyethylene glycol (PEG) is a non-toxic, non-immunogenic biomaterial that has been shown to be resistant to non-specific protein adsorption and undesired interactions with cells.[12,13] These properties have led to its wide use in biotechnology and medicine *e.g.* non-fouling coatings and PEGylation for drug delivery. Interestingly, it is this very stealth property of PEG that makes it a remarkably excellent substrate for cell behavior studies. One of the main advantages of PEG is that it provides researchers with the ideal, inert background for cell studies, where interactions with the surface modifications can be investigated with minimal unwanted interference from the substrate.[7,14–18] Nevertheless, although reported to be highly cell repellent, when patterned topographically or elastically, cells do in fact interact with and adhere to the PEG surface, as we have recently discovered.[19–21]

[a]Technische Universität Berlin, Department of Chemistry, Nanostrukturierte Biomaterialien, Sekr. TC 1, Straße des 17. Juni 124, 10623 Berlin, Germany. E-mail: Lensen@Chem.TU-Berlin.de

[b]Technische Universität Berlin, Department of Chemistry, Sekr. TK 01, Straße des 17. Juni 135, 10623 Berlin, Germany

† Electronic supplementary information (ESI) available. See DOI: 10.1039/c3tc30811a

‡ Present address: Australian Future Fibres Research & Innovation Centre, Institute for Frontier materials, Deakin University, Geelong, Australia.

§ Present address: Surface Science Group, Biomedical Diagnostics Institute, Dublin City University, Dublin 9, Ireland.

Efficient and fast crosslinking methods can be used to make PEG hydrogel networks from PEG-macromonomers. For example, photo-polymerization of polyethylene glycol diacrylate (PEGDA) liquid precursors allows not only the resulting hydrogel to be molded into any desired shape but also enables the control over crosslinking density – dependent on the amount of photoinitiator and eventual low-molecular weight crosslinker used – and therefore the stiffness of the material. Based on this flexibility, our group has fabricated patterned substrates of PEG comprised of topographies with resolution even in the sub-10 nm range[22] and has designed the patterning technique FIMIC (Fill Molding in Capillaries) to prepare topographically smooth, micro-sized patterns of tunable elasticity using PEG of various compositions.[23]

Cells have been shown to react not only to micro-structures and micro-environments but, as has been more recently discovered, to nano-topographies and chemical nano-patterns as well.[24] In particular, gold nanoparticles (Au NPs) have been employed in nano-patterning of surfaces including silicon and polymeric biomaterials such as hydrogels. From the wide variety of available inorganic nanoparticles, Au NPs in particular are chosen since they can anchor bio-functional molecules containing thiol (–SH) groups selectively and reliably *via* the thiol functionality, and thus provide accurately controlled, chemical cues for the cells. These factors, *i.e.* the nanoscopic arrangement and the selective bio-functionalization, have proven to be of vital importance in enabling cell adhesion, spreading and consequent viability on these surfaces.[25] The fabrication of orderly arranged Au NPs from block copolymer templates on surfaces namely allows for the accurate positioning of single molecules on a surface in a pre-defined ordered pattern, which then enables the systematic study into the influence of the density and distribution of certain extracellular matrix (ECM) molecules on cell behavior, at the biointerface.[26,27]

In this paper we take our previously developed surface patterning methods to the next level by combining chemical patterning *via* Au NP functionalization, and physical patterning *via* PEG hydrogel micro-topographies (Fig. 1). Those bi-functional patterns should provide physical confinement for the cells between the PEG microbars so that they can then be locally stimulated by the chemical pattern on the Au NP template with nanoscopic precision.

The fabrication of these model structures for cell stimulation studies involves two main procedures. First, micro-sized lines of ordered Au NPs are obtained on silicon wafers *via* a block copolymer micelle (BCM) patterning method called micro-contact deprinting (μ-CdP), which was recently developed by our group.[28] This method employs polymer stamps to remove Au NP precursors in a polymeric template from a surface and can be easily accomplished in an ordinary research lab without the need for any expensive facilities. μ-CdP also offers a high efficiency for the preparation of large area patterns (around 1 cm^2), which is advantageous for cell studies, and can even be applied on curved surfaces. The second step in the production of the hybrid structures involves the decoration of the now Au NP-patterned (silicon or glass) surface with acrylate groups *via* silanization, onto which patterns of PEG bars are adhesively embossed, *via* PEGDA MicroMolding in Capillaries (MIMIC) followed by photopolymerization.[29,30]

Beside the high degree of control of the positioning of the nanostructures, another advantage of this method is that, in addition to silicon surfaces, the versatility of the adhesive embossing procedure allows the complex patterning of different substrates including glass and even PEG-based hydrogels as we have discovered, both of which provide a transparent substrate for use in cell culture and optical microscopy.

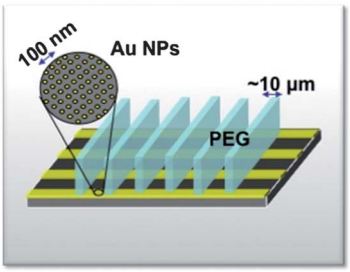

Fig. 1 Schematic illustration of the bi-functional nano-/micro-pattern composed of Au NPs (lines) and grafted PEG bars.

Experimental

Orderly arranged Au NPs on a silicon wafer

The procedure is known as block copolymer micelle nanolithography.[31,32] Self-assembled micelles of PS(1653)-*b*-P2VP(400) with $HAuCl_4$ salt in the micellar core were first prepared in a selective solvent. In detail, the block copolymer (Polymer Source Inc.) was first dissolved in dry toluene (5 mg mL^{-1}) and after stirring for 48 h allowing the formation of micelles, gold(III) chloride, $HAuCl_4 \cdot 3H_2O$ (Aldrich), was added to the solution (0.3 equiv. of Au(III) per pyridine unit) and stirred for another 24 h at room temperature under exclusion of light. The gold salt-loaded block copolymer micelles (Au-BCM) were deposited onto the surface of a silicon wafer in a well-ordered monolayer *via* dip-coating, at a withdrawal speed of 10 mm min^{-1}. The micelle-covered silicon wafers (Au-BCM@Si, around 1 × 1 cm^2) were then treated with hydrogen plasma (machine: PVA TePla 100) for 1 h (100 W, 0.05 mbar) in order to both burn off the polymer micelles and reduce the salt in the core of micelles into Au NPs at the same time.

Micro-contact deprinting (μ-CdP)

"Micro-contact deprinting" was carried out according to the procedure reported in our previous publication.[28] On a freshly prepared monolayer of block copolymer micelles deposited on a substrate as introduced above (Au-BCM@Si), a topographically micro-patterned polystyrene (PS) stamp heated at 140 °C was applied and removed again after several seconds of contact, in order to selectively peel off selected areas of the underlying Au-BCM monolayer, through conformal contact between the PS micro-topography and the micelles, resulting in an Au-BCM micro-patterned substrate, with an inverse pattern motif with

respect to the PS topography. After deprinting, the micelle-patterned silicon wafers (Au-BCM@$Si_{\mu\text{-CdP}}$) were treated with hydrogen plasma as described above yielding micro-patterns of Au NP arrays (Au-NP@$Si_{\mu\text{-CdP}}$).

Silanization of the substrate

Immediately after the plasma treatment, the Au-NP-patterned silicon wafers (Au-NP@Si or Au-NP@$Si_{\mu\text{-CdP}}$) were put into a desiccator together with a vial containing several drops of 3-(trimethoxysilyl) propyl methacrylate (TMSPMA). The desiccator was evacuated and sealed, allowing the vapor of TMSPMA to fill the desiccator and to chemisorb at the surface of the Si wafer. After two hours the silicon wafers were taken out, washed in 20 mL of dry toluene 3 times to remove unreacted TMSPMA from the surface and dried under a flow of nitrogen.

Adhesive embossing (adapted from the MIMIC-method)

1 Preparation of PDMS molds. PDMS molds with micro-patterns of lines (3–50 μm in width) were prepared by replication from silicon masters. The PDMS precursor mixture (Sylgard 184, Dow Corning, 10 : 1) was poured without further modification on the surface of the silicon masters and placed under vacuum to remove the air bubbles from the micro-capillaries. Finally the PDMS filled Si masters were cured at 120 °C for 2 h. The solidified PDMS molds were peeled off from the silicon master and cut into pieces of around 1 cm^2.

2 Adhesive embossing. To affix bars of PEG onto the surface of the Au-NP-patterned silicon wafer, first, a piece of PDMS mold containing micro-capillaries was sealed tightly to the surface of the silicon wafer. Next, a small droplet of polyethylene glycol diacrylate (PEGDA, Mn 575) precursor mixed with 1 wt% of photoinitiator IRGACURE 2959 was deposited at the entrance of the micro-channels of the PDMS mold. After the channels were completely filled by capillary action, the assembly of silicon wafer and PEGDA filled PDMS mold was cured with UV light (365 nm, 6 W) in a glove box filled with nitrogen for 30 min. Finally the PDMS mold was removed carefully with tweezers, leaving behind the cured inverse PEG-structures on the silicon surface. It was verified by AFM and SEM that the PDMS mold did not leave a print of contaminations or removed Au NPs from the surface.

3 Electroless gold plating. The electroless plating experiment was performed as follows. The respective substrates were immersed in aqueous gold growth precursor solutions composed of (0.1% w/w) $HAuCl_4 \cdot 3H_2O$ and (0.2 mM) $NH_2OH \cdot HCl$ as reducing agent. After 3 minutes of immersion time, the substrates were taken out, rinsed with water, isopropanol and acetone and then blown dry with nitrogen.

Scanning probe microscopy

Atomic force micrographs were recorded with a Digital Instruments Multimode equipped with a Nanoscope IIIa controller (Veeco Instruments, Santa Barbara, CA). Imaging was done in the tapping mode using standard silicon cantilevers (k_40 N m^{-1}, $f = 300$ kHz; Nanoworld, Neuchatel, Switzerland). Images were edited with Nanoscope software (v5.12r5 Digital Instruments, Veeco, Santa Barbara, CA).

Scanning electron microscopy

The resulting structures were investigated in a dry state using a field emission scanning electron microscope (FESEM, Hitachi model S-4800 and JEOL model F7401 with an in-lens secondary electron detector).

Results and discussion

The strategy to prepare bi-functional micro- and nano-patterns of Au NP arrays and PEG microbars on hard substrates, *e.g.* silicon, is a combination of two patterning procedures (Fig. 2). First, monolayers of gold salt loaded block copolymer micelles (Au-BCM) are deposited *via* dip-coating onto the surface of a silicon wafer (Au-BCM@Si), followed by the selective removal of defined patterns of these micelles *via* "micro-contact deprinting" using a micro-molded polystyrene (PS) stamp (Au-BCM@$Si_{\mu\text{-CdP}}$), concluded by plasma treatment, which converts the gold salt loaded micelles into gold nanoparticles; Au-NP@$Si_{\mu\text{-CdP}}$.[28] These steps are schematically depicted in Fig. 2, I. Secondly, micro-bars of a PEG hydrogel are adhesively embossed onto the now Au NP-patterned silicon substrate (Fig. 2, II) using the soft lithographic method MIMIC (Micro-Molding in Capillaries).[29] The final product is denoted as Au-NP@$Si_{\mu\text{-CdP}}$ + PEG_{MIMIC}.

In the very first step of this fabrication procedure (Fig. 2, I), we want the Au NPs to be arranged in an ordered, periodic structure on the silicon wafer. This is carried out using block copolymer micelle nanolithography, which allows the deposition of close-packed monolayers of (gold precursor loaded) block copolymer micelles (Au-BCM) *via* dip-coating onto the substrate and thus allows the formation of hexagonally ordered Au NP arrays on the silicon substrate (Au-NP@Si), as evidenced

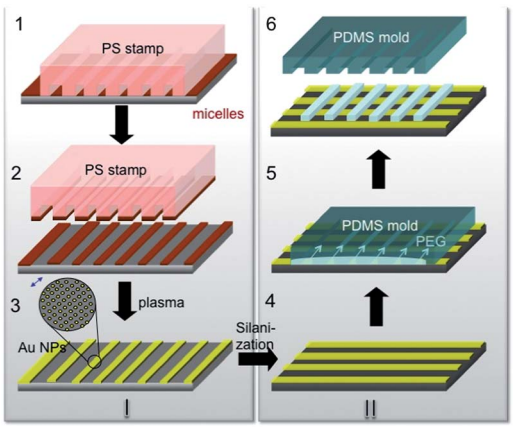

Fig. 2 Schematic illustration of the fabrication of PEG/Au NP hierarchical patterns on the surface of a silicon wafer (Au-NP@$Si_{\mu\text{-CdP}}$ + PEG_{MIMIC}): (I) micro-sized lines consisting of Au NPs were obtained on the silicon wafer *via* micro-contact deprinting (μ-CdP); (II) PEG-microbars were fabricated on the surface of the Au NP patterns through MIMIC (using PDMS molds), after appropriate silanization of the substrate.

in the scanning electron micrograph in Fig. 3a. To get further insight, complementary atomic force microscopy (AFM) measurements were performed. From AFM inspection, a particle size of 10 nm and particle spacing of 90 nm on average could be determined (image not shown). The "micro-contact deprinting" method results in the clean removal of micro-lines of the arranged micelles (Au-BCM). Fig. 3b shows a detail of the eventual substrate Au-NP@$Si_{\mu\text{-CdP}}$ (*i.e.* after plasma cleaning of the deprinted samples). It can be seen that the Au-BCM have been tracelessly removed from the area where the PS stamp had been in contact, resulting in a sharp transition between Au NP decorated areas and clean silicon areas.

For the firm adhesion of the PEG microbars onto the micro-patterned silicon substrate with Au NP arrays, the accessible gold-free silicon surface on the Au-NP@$Si_{\mu\text{-CdP}}$ substrate is functionalised with acrylate groups (Fig. 2, between processes I and II) in order to (1) increase the wettability of the PEGDA precursor onto the silicon substrate and thus favoring the capillary filling of the PDMS mold in the "adhesive embossing" process and (2) to ensure strong surface attachment of the PEG bars obtained after curing, *via* surface-to-bulk cross-linking. Thus, a silane derivative bearing methacrylate groups (TMSPMA) was chosen to modify the silicon surface. The silicon surface is easy to modify with TMSPMA at this stage, as the plasma treatment used in the previous step conveniently activates the surface of the silicon substrate for chemical vapor deposition of silane precursors.

The presence of methacrylate groups on the surface of the silicon substrate played a key role in the "adhesive embossing" process (Fig. 2, process II). Indeed, with the organic primer layer present, the intrusion of the liquid PEG precursor into the channels of the PDMS mold was greatly accelerated when compared with the surface of the unmodified silicon wafer, probably due to an increased wettability of the PEG precursor onto the acrylated silicon surface. When the adhesive embossing of PEG bars was carried out in the absence of surface acrylate groups, successful adhesion still occurred. However, especially for bars with high aspect ratio, a significant number of PEG bars were inadvertently removed together with the PDMS mold, indicating a weaker surface attachment of the PEG structures. Besides, the PEG bars that did remain on the non-functionalized silicon wafers were shown to detach from the surface upon PEG swelling in water. This further evidences the necessity of surface-to-bulk cross-linking during curing to achieve a strong surface anchorage of the PEG structures, which is a prerequisite for subsequent cell studies in aqueous environments.

Provided that there are sufficient reactive groups on the surface, the process of "adhesive embossing" works on any surface. Accordingly, PEG microbars could be successfully attached to glass modified with a TMSPMA primer layer (see Fig. 4a) and even to self-supported PEG-based hydrogel films (see Fig. 4b and c). In the latter case, the covalent adhesion of the embossed PEG bars is achieved through surface-to-bulk cross-linking *via* the remaining acrylate groups on the surface of the PEG-based hydrogel films, resulting from incomplete UV-curing. Especially the possibility to attach PEG microstructures of a certain composition to smooth PEG hydrogel films with a different composition is extremely interesting for the generation of micro-structured elasticity patterns for cell studies. Indeed, the stiffness of the respective PEG components largely

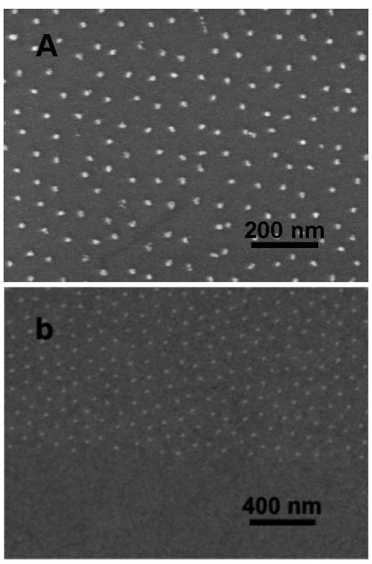

Fig. 3 (a) SEM image of Au-NP@Si showing orderly arranged Au NPs; (b) FESEM image of a detail of a Au-NP@$Si_{\mu\text{-CdP}}$ sample exhibiting lines consisting of orderly arranged Au NPs (here the pattern consists of lines of Au NPs of 3 μm width and 10 μm spacing).

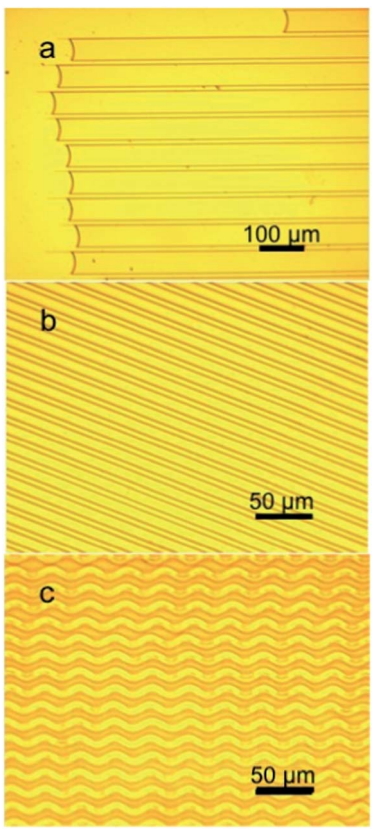

Fig. 4 PEG microbars fabricated by "adhesive embossing" on transparent base substrates; (a) PEG microbars on glass; (b) PEG microbars on a PEG-substrate ("PEG-on-PEG") and (c) a PEG-on-PEG sample after swelling in water.

depends on the degree of cross-linking, which is controlled by the amount of photo-initiator and curing time. Thus, using this approach, two-component PEG based micro-patterns, with mutually different mechanical properties, *e.g.* topographic structures of softer PEG-hydrogels attached to stiffer PEG substrates or *vice versa*, can be generated. In Fig. 4c, the effect of swelling of such a two component "PEG-on-PEG" micro-pattern is illustrated, highlighting the firm adhesion of the PEG micro-structures. While after adhesive embossing in the absence of a solvent, a linear PEG–PEG micro-pattern is observed (Fig. 4b), the differential swelling of the two PEG components (bars and substrate) results in a wavy appearance of the microbars after incubation in water.

Building on this knowledge that we can adhere micro-bars of PEG to various substrates, we set about fabricating the bi-functional nano-/micro-patterns consisting of PEG bars on silicon patterned with Au NPs, *i.e.* first Au-NP@Si + PEG_{MIMIC} and eventually Au-NP@$Si_{\mu\text{-}CdP}$ + PEG_{MIMIC}. To begin with we adhered PEG lines that were 10 μm in width, 3 μm in spacing, and 5 μm in height onto a silicon surface coated with a homogeneous periodic array of Au-NPs (Fig. 5a and b). An image at higher magnification (Fig. 5b) shows the details of the area between two PEG bars, where the Au NP array can be clearly recognized.

Following on from the simple hybrid patterns, more complex patterns were successfully obtained, where rather than employing a silicon wafer decorated with a homogeneous coverage of Au NPs (Au-NP@Si) as substrate for the adhesive embossing process (to yield Au-NP@Si + PEG_{MIMIC} samples (Fig. 5a and b)), we performed the micro-contact deprinting step prior to the adhesive embossing. PEG bars were successfully adhered to the now Au NP-patterned surfaces giving unusual layers of nano- and micro-patterning in one substrate. Fig. 5c and d exhibit images of the complex perpendicular and oblique patterns of PEG and Au NPs (Au-NP@$Si_{\mu\text{-}CdP}$ + PEG_{MIMIC}) that were thus obtained.

One of the most impressive patterns achieved was of high aspect ratio (6) PEG bars whose height will provide effective barriers for the confinement of cells on the surface (adhering to the Au NP-patterned surface). Here we show PEG lines of 17 μm height, 3 μm width that are 20 μm spaced on both Au-NP@Si + PEG_{MIMIC} and Au-NP@$Si_{\mu\text{-}CdP}$ + PEG_{MIMIC} surfaces (Fig. 6). The fabrication of such high aspect ratio patterns constitutes a big challenge to researchers as many defects may appear during fabrication, such as broken or collapsed patterns as well as partly missing patterns that were peeled-off together with the mold.

Nonetheless, the robustness of the high aspect ratio PEG bars is evident in images (b) and (d) in Fig. 6 where the proceeding edge of the PEG liquid precursor can be seen (the peculiar lines that are ahead of the filling front are inherent to the MIMIC-process and were also observed in the original report by Whitesides *et al.*).[29] Now cured, this PEG hydrogel

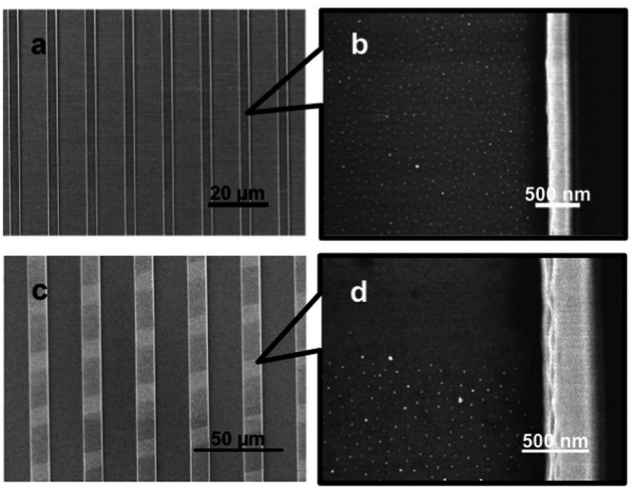

Fig. 5 SEM images of Au NP-PEG complex patterns with PEG microbars of 5 μm in height, of certain width distance (μm): (a and b) 3–10 μm PEG bars on Au NPs (Au-NP@Si + PEG_{MIMIC}); and (c and d) 10–20 μm PEG bars over Au NP lines of 20–10 μm(Au-NP@$Si_{\mu\text{-}CdP}$ + PEG_{MIMIC}).

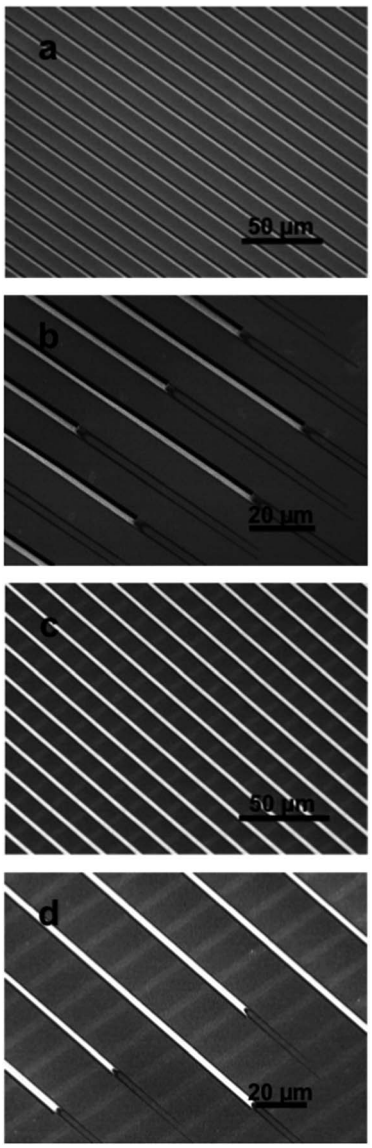

Fig. 6 FESEM images of complex patterns with PEG lines of high aspect ratio (3 μm in width, 20 μm in distance, and 17 μm in height) on (a and b) continuous Au NPs (Au-NP@Si + PEG_{MIMIC}); (c and d) Au NP lines of 3 μm width with the spacing of 10 μm (Au-NP@$Si_{\mu\text{-}CdP}$ + PEG_{MIMIC}).

stands strong and unwavering against the silicon backdrop, a property accredited to the strength of the bond between the acrylate groups in the gel and on the silicon surface.

In our complex and hybrid patterns, we intend to use the Au NPs present on the surface as anchor points for the accurate positioning of bio-functional molecules. For this reason, the surface of the Au NPs must be accessible for surface functionalization, after all the involved steps such as surface acrylation and PDMS contact required for the adhesive embossing (MIMIC) process. To prove that the PDMS mold did not affect the Au NP surface accessibility, we investigated the Au NPs located along the micro-lines of the sample after PEG bar adhesion (Au-NP@Si + PEG) with atomic force microscopy (AFM). In the AFM image of the Au NPs present in the final hybrid pattern, no obvious changes could be detected when compared with AFM images of Au NPs on the starting substrate, *i.e.* before silanization and MIMIC (Au-NP@Si or Au-NP@$Si_{\mu\text{-}CdP}$; images not shown). This already indicates that the further process does not affect the Au NPs.

To further verify the availability of Au NPs for functionalisation, even after surface modification, we carried out an electroless plating experiment. After submersion of an Au NP-patterned silicon wafer (Au-NP@Si modified with TMSPMA and after having been in contact with a PDMS stamp) in an electroless plating bath for 3 min, the area with Au NPs was covered with gold nanoparticles of ~50 nm while bare silicon wafer control samples were practically unchanged, proving that the Au NPs are still available for functionalization, in this case acting as seeds for gold deposition (images shown in Fig. S1 in the ESI†).

Conclusions

A method was developed to prepare hybrid surface patterns, composed of micro-sized topographic structures of PEG bars and micro-sized patterns of nano-ordered Au NPs. Significant steps have been taken in the patterning of high aspect ratio polymer patterns that can act as physical barriers to guide cell adherence and migration, with a factor of 6 being achieved so far. Alongside these physical cues, chemical cues are provided by ordered arrays of Au NPs that will be further exploited as anchors for binding bio-functional molecules. These complex hybrid patterns will provide versatile *in vitro* platforms for the study of cellular responses which can mimic the complex *in vivo* microenvironment *e.g.* they can be used to study the competition between the influences of a variety of physical cues and specific chemical cues.

Acknowledgements

The authors greatly acknowledge funding in the form of a Sofja Kovalevskaja Award granted to M. C. Lensen by the Alexander von Humboldt foundation and the funding by the Federal Ministry for Education and Research (BMBF) and thank the Deutsche Forschungsgemeinschaft (DFG) for financial support within the framework of the German Initiative for Excellence the Cluster of Excellence "Unifying Concepts in Catalysis" (EXC 314) coordinated by the Technische Universitaet Berlin. The authors also would like to express gratitude to DWI an der RWTH Aachen e.V. for the support in materials and facilities.

Notes and references

1 D. A. Puleo and R. Bizios, *Biological Interactions on Materials Surfaces: Understanding and Controlling Protein, Cell, and Tissue Responses*, Springer-Verlag, New York, 2009.
2 S. Kizilel, V. H. Perez-Luna and F. Teymour, *Langmuir*, 2004, **20**, 8652–8658.
3 M. S. Hahn, L. J. Taite, J. J. Moon, M. C. Rowland, K. A. Ruffino and J. L. West, *Biomaterials*, 2006, **27**, 2519–2524.
4 Y. L. Wang, G. T. Salazar, J. H. Pai, H. Shadpour, C. E. Sims and N. L. Allbritton, *Lab Chip*, 2008, **8**, 734–740.
5 M. C. Lensen, P. Mela, A. Mourran, J. Groll, J. Heuts, H. T. Rong and M. Moller, *Langmuir*, 2007, **23**, 7841–7846.
6 A. Verma, A. Sharma and G. U. Kulkarni, *Small*, 2011, **7**, 758–765.
7 J.-H. Kim, S. Seo and J. Min, *J. Biotechnol.*, 2011, **155**, 308–311.
8 D. Liazoghli, A. D. Roth, P. Thostrup and D. R. Colman, *ACS Chem. Neurosci.*, 2011, **3**, 90–95.
9 K. Y. Suh and R. Langer, *Appl. Phys. Lett.*, 2003, **83**, 1668–1670.
10 K. Y. Suh, J. Seong, A. Khademhosseini, P. E. Laibinis and R. Langer, *Biomaterials*, 2004, **25**, 557–563.
11 H. W. Shim, J. H. Lee, T. S. Hwang, Y. W. Rhee, Y. M. Bae, J. S. Choi, J. Han and C. S. Lee, *Biosens. Bioelectron.*, 2007, **22**, 3188–3195.
12 M. J. Harris, in *ACS symposium series*, ed. S. Zalipsky and J. M. Harris, American chemical Society, 1997, vol. 680.
13 M. J. Roberts, M. D. Bentley and J. M. Harris, *Adv. Drug Delivery Rev.*, 2002, **54**, 459–476.
14 S. Nemir, H. N. Hayenga and J. L. West, *Biotechnol. Bioeng.*, 2010, **105**, 636–644.
15 K. Yoshimoto, M. Ichino and Y. Nagasaki, *Lab Chip*, 2009, **9**, 1286–1289.
16 M. R. Hynd, J. P. Frampton, N. Dowell-Mesfin, J. N. Turner and W. Shain, *J. Neurosci. Methods*, 2007, **162**, 255–263.
17 J. Y. Jeffrey, M. Karp, G. Eng, J. Fukuda, J. Blumling, K.-Y. Suh, J. Cheng, A. Mahdavi, J. Borenstein, R. Langer and A. Khademhosseini, *Lab Chip*, 2007, **7**, 786–794.
18 H. J. Lee, H.-S. Kim, H. O. Kim and W.-G. Koh, *Lab Chip*, 2011, **11**, 2849–2857.
19 V. A. Schulte, M. Diez, M. Möller and M. C. Lensen, *Biomacromolecules*, 2009, **10**, 2795–2801.
20 V. A. Schulte, M. Diez, Y. Hu, M. Möller and M. C. Lensen, *Biomacromolecules*, 2010, **11**, 3375–3383.
21 M. Diez, V. A. Schulte, F. Stefanoni, C. F. Natale, F. Mollica, C. M. Cesa, J. Chen, M. Möller, P. A. Netti, M. Ventre and M. C. Lensen, *Adv. Eng. Mater.*, 2011, **13**, B395–B404.
22 M. Diez, P. Mela, V. Seshan, M. Moller and M. C. Lensen, *Small*, 2009, **5**, 2756–2760.
23 S. Kelleher, A. Jongerius, A. Loebus, C. Strehmel, Z. Zhang and M. C. Lensen, *Adv. Eng. Mater.*, 2012, **14**, B56–B66.
24 M. Dalby, N. Gadegaard, R. Tare, A. Andar, M. Riehle, P. Herzyk, C. Wilkinson and R. Oreffo, *Nat. Mater.*, 2007, **6**, 997–1003.

25 M. Arnold, E. A. Cavalcanti-Adam, R. Glass, J. Blummel, W. Eck, M. Kantlehner, H. Kessler and J. P. Spatz, *ChemPhysChem*, 2004, **5**, 383–388.
26 M. S. Marco Arnold, J. Blümmel, E. A. Cavalcanti-Adam, M. López-García, H. Kessler, B. Geigerc and J. P. Spatz, *Soft Matter*, 2009, **5**, 72–77.
27 M. S. Daniel Aydin, I. Louban, S. Knoppe, J. Ulmer, T. L. Haas, H. Walczak and J. P. Spatz, *Small*, 2009, **9**, 1014–1018.
28 J. Y. Chen, P. Mela, M. Moller and M. C. Lensen, *ACS Nano*, 2009, **3**, 1451–1456.
29 E. Kim, Y. N. Xia and G. M. Whitesides, *J. Am. Chem. Soc.*, 1996, **118**, 5722–5731.
30 J. F. Kauffman, S. J. Gilliam and R. S. Martin, *Anal. Chem.*, 2008, **80**, 5706–5712.
31 J. P. Spatz, S. Mossmer, C. Hartmann, M. Moller, T. Herzog, M. Krieger, H. G. Boyen, P. Ziemann and B. Kabius, *Langmuir*, 2000, **16**, 407–415.
32 G. Kastle, H. G. Boyen, F. Weigl, G. Lengl, T. Herzog, P. Ziemann, S. Riethmuller, O. Mayer, C. Hartmann, J. P. Spatz, M. Moller, M. Ozawa, F. Banhart, M. G. Garnier and P. Oelhafen, *Adv. Funct. Mater.*, 2003, **13**, 853–861.